Robot Aided Passive Rehabilitation using Nonlinear Control Techniques

M. H. Rahman[1, 2], P. S. Archambault[1]
[1]School of Physical & Occupational Therapy,
McGill University, and Center for Interdisciplinary
Research in Rehabilitation (CRIR), Montréal, Canada
mhrahman@ieee.org, philippe.archambault@mcgill.ca

M. Saad, C. O. Luna, S. B. Ferrer
Department of Electrical Engineering
[2]École de technologie supérieure (ETS), Montréal, Canada
maarouf.saad@etsmtl.ca, cristobal.ochoa-luna.1@ens.etsmtl.ca, steven.ferrer.1@ens.etsmtl.ca

***Abstract*—This paper presents a robot aided passive arm movement therapeutic scheme. A seven DoFs robot, *ETS-MARSE* (motion assistive exoskeleton robot for superior extremity) was used for this purpose. It is an exoskeleton type wearable robot, which was designed corresponds to human upper-limb biomechanics, to provide movement assistance and rehabilitation to the individuals with upper limb dysfunction due to conditions such as stroke or spinal cord injuries. Considering the dynamic modeling of the exoskeleton which is nonlinear in nature, we have employed nonlinear control techniques (sliding mode and computed torque) to maneuver the exoskeleton. Experiments were carried out with healthy male human subjects where trajectories tracking in the form of passive rehabilitation exercises were performed.**

Keywords—ETS-MARSE; trajectory tracking; passive rehabilitation; sliding mode control; computed torque control

I. INTRODUCTION

The Canadian Stroke Network reports that fifty thousand Canadians suffer from strokes each year, and over 300,000 Canadians are currently living with the effects of a stroke [1]. In the United States, it is more than 795,000 individuals who suffer strokes each year [2] The majority of stroke survivors live with long-term disabilities leading to serious social and economic impacts: it is estimated that stroke and heart diseases cost Canada more than $22.2 billion annually [2]. This cost burden is more than double in the United States which is estimated $54 billion annually [3]. These numbers will continue to rise as the population continues to age.

Between 30 and 66% of stroke survivors have persistent deficits in upper extremity function six months after stroke [4]. This results in a burden on their families, communities and society as well. Rehabilitation programs which required skilled therapists or clinicians has been playing key role in promoting functional recovery in these subjects. However, since the number of such cases is constantly growing and the treatment duration is long, introducing robots could therefore significantly contribute to the success of these programs. Recent studies reveal that patients who receive robot-assisted therapy show considerable improvement of motor skills compared to conventional therapy techniques [5].

To provide rehabilitation therapies, these robots mechanically interface with human arm movements. Two types of such mechanical robots are considered: *end effector robots* act on the human arm on one point, usually the hand or forearm, while *exoskeleton robots* are worn over the arm and can act at multiple joints. In our previous researches, we developed a 3DoFs exoskeleton robot, *ExoRob* for elbow and wrist joint movement assistance [6]. Later on, we developed a 4DoFs *ExoRob* for assisting shoulder and elbow joint movements [7], and a 5DoFs exoskeleton robot, *MARSE-5* for shoulder, elbow and forearm movement supports [8]. In a continuing effort toward providing movement assistance to the whole arm (shoulder, elbow, forearm, and wrist joint), as well as to provide effective rehabilitation therapy in all joints' movements, we recently developed a 7DoFs robotic exoskeleton, *ETS-MARSE*. It is to be noted that, though the *ETS-MARSE* was developed with the goal of providing different forms of rehabilitation therapy (e.g., passive arm movement therapy, and/or active rehabilitation therapy), this paper focused only on the passive form of rehabilitation.

The passive arm movement therapy is the very first type of physiotherapy treatment (exercise) given to the patients to improve passive range of movements. This exercises are usually performed slowly [9] compared to the natural speed of arm movement. In this research we formed a library of exercises (in the form reference/command trajectories for the *ETS-MARSE*) with the typical passive rehabilitation exercises (for single and multi joint movements e.g., elbow flexion/extension or reaching task etc) recommended by the clinicians and therapists.

As a control strategy, to drive the *ETS-MARSE* in providing passive arm movement therapy, we have used nonlinear control techniques, s*liding mode control* (SMC) and *computed torque control* (CTC). These are model based control approaches which include the dynamic model of the system (in this case model of human upper-limb and the *ETS-MARSE*). Therefore, it is expected that they will give better tracking performance compared to the linear control techniques such as a PID control, as long as the dynamic modeling of the system is perfect. It is to be mentioned here that the dynamic modeling of human arm movement is nonlinear in nature, so it was justified using nonlinear control techniques. Among the nonlinear control approaches, CTC is simple to design and takes less computation. On the other hand, SMC technique is considered as a robust control technique which theoretically ensures perfect tracking despite of parameter or model uncertainties [10]. We therefore considered SMC and CTC as good solutions to deliver a consistently high dynamic tracking performance. Experiments were carried out with healthy human subjects. In experiments,

978-1-4673-5769-2/13/$31.00 ©2013 IEEE

trajectory tracking (i.e., pre-programmed trajectory from the library of exercises) that corresponds to typical rehabilitation (passive) exercises [11] of the shoulder, elbow, forearm and wrist joint movements were carried out to evaluate performances of the *ETS-MARSE* and the controllers.

In the next section of this paper, an overview of the development of the *ETS-MARSE* is presented. Section III describes the control strategies. In section IV, experimental results are presented to evaluate the performance of the *ETS-MARSE* with regard to passive rehabilitation, and finally, the paper ends with the conclusion and future works in section V.

II. Upper Limb Exoskeleton Robot, *ETS-MARSE*

The *ETS-MARSE* as shown in Fig. 1 has 7DoFs and is able to provide every variety of movements to the upper extremities (UE). It was designed correspond to the natural range of a human UE. Its shoulder joint has 3DoFs which assists in horizontal & vertical flexion/extension, and internal/external rotation. Its elbow joint is modeled as hinge joint and is responsible for elbow flexion/extension. The forearm motion support part (1DoF) is responsible for pronation/supination, and the wrist motion support part (which has 2DoFs) is responsible for radial/ulnar deviation and flexion/extension of wrist joint. The *ETS-MARSE* was designed for typical adult. It was fabricated with aluminum to give the exoskeleton structure a relatively light weight. Provision included in the design to adjust the link-lengths to accommodate a wide range of individuals. Brushless DC motors (Maxon EC45, EC90) were used to actuate the *ETS-MARSE*.

III. Control

In this paper, we have employed two nonlinear control techniques (CTC and SMC) in dynamic trajectory tracking of the *ETS-MARSE*.

A. Computed Torque Control (CTC)

The general layout of the computed torque control technique is depicted in Fig. 2. Unlike the conventional computed torque control approach, here we have added an integral term to have a better tracking performance and to compensate the trajectory tracking error that usually occurs due to imperfect dynamic modeling, parameter estimation, and also for external disturbances.

The dynamic behaviour of the *ETS-MARSE* can be expressed by the well-known rigid body dynamic equation as:

$$M(\theta)\ddot{\theta} + V(\theta,\dot{\theta}) + G(\theta) + F(\theta,\dot{\theta}) = \tau \qquad (1)$$

where τ is the generalized torques vector, $M(\theta) \in \mathbb{R}^{7\times7}$ is the inertia matrix, $V(\theta,\dot{\theta}) \in \mathbb{R}^7$ is the coriolis/centrifugal vector, $G(\theta) \in \mathbb{R}^7$ is the gravity vector, and $F(\theta,\dot{\theta}) \in \mathbb{R}^7$ is the friction vector. Note that the friction vector is modeled as a nonlinear coulomb friction, and can be expressed as:

$$\tau_{friction} = F(\theta,\dot{\theta}) = c\, sgn(\dot{\theta}) \qquad (2)$$

where c is the coulomb-friction constant. Equation (1) can be written as:

$$\ddot{\theta} = -M^{-1}(\theta)\left[V(\theta,\dot{\theta}) + G(\theta) + F(\theta,\dot{\theta})\right] + M^{-1}(\theta)\tau \qquad (3)$$

$M^{-1}(\theta)$ always exists since $M(\theta)$ is symmetrical and positive definite. The control torque in Fig. 2 can be written as:

$$\tau = M(\theta)\left[\ddot{\theta}_d + K_v(\dot{\theta}_d - \dot{\theta}) + K_p(\theta_d - \theta) + K_i\int(\theta_d - \theta)\,dt\right] + V(\theta,\dot{\theta}) + G(\theta) + F(\theta,\dot{\theta}) \qquad (4)$$

From relations (1) and (4), we may write:

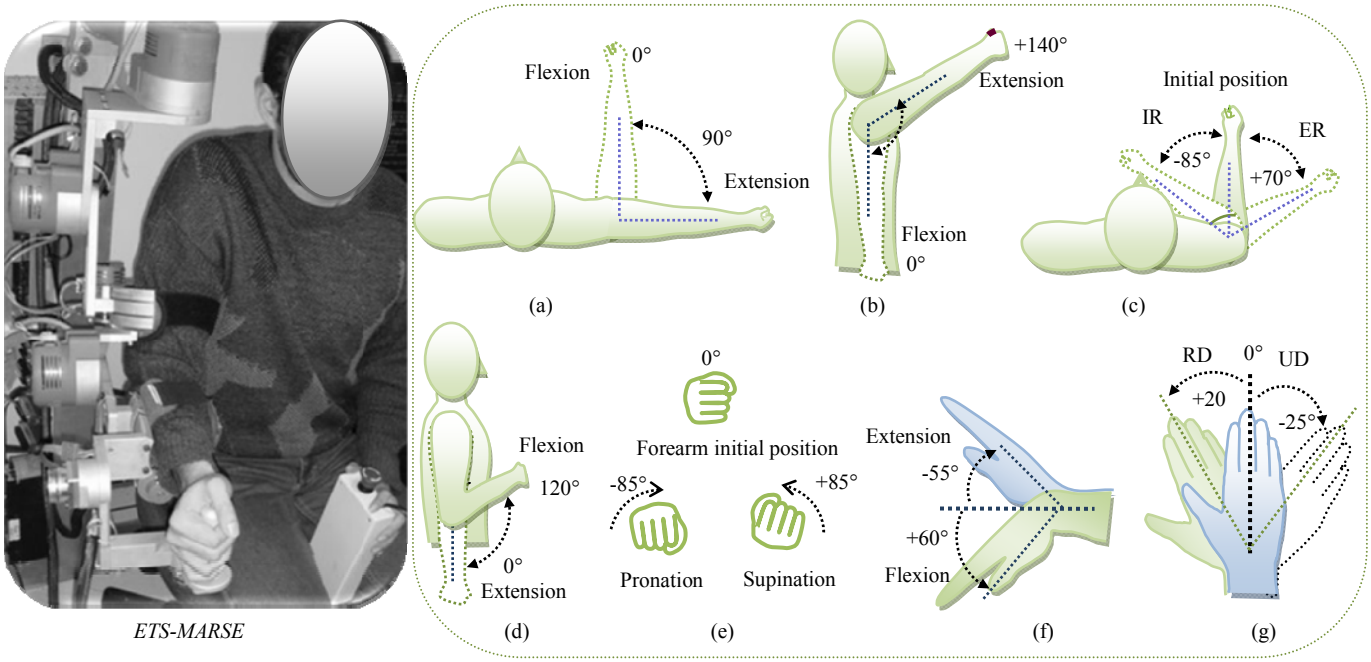

Fig. 1. *ETS-MARSE* and its joint range of motion. (a) Shoulder joint: horizontal flexion / extension; (b) Shoulder joint: vertical flexion / extension; (c) Shoulder joint: internal rotation (IR) / external rotation (ER); (d) Elbow: flexion / extension; (e) Forearm: pronation / supination; (f) Wrist: flexion / extension; (g) Wrist: radial deviation (RD) / ulnar deviation (UD).

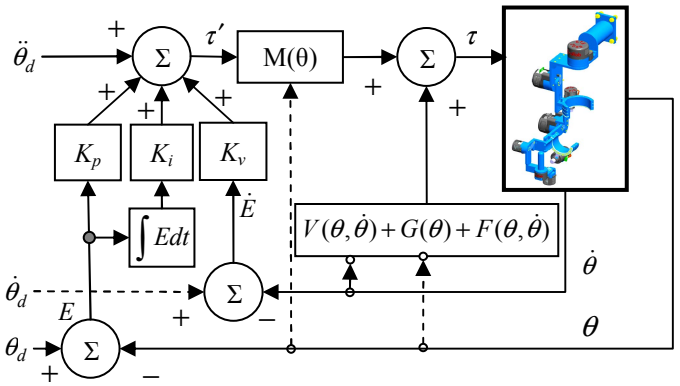

Fig. 2. Schematic diagram of computed torque control

$$\ddot{\theta} = \ddot{\theta_d} + K_v(\dot{\theta}_d - \dot{\theta}) + K_p(\theta_d - \theta) + K_i \int (\theta_d - \theta)\, dt \tag{5}$$

where, $\theta_d, \dot{\theta}_d,$ and $\ddot{\theta}_d$ are the desired position, velocity and acceleration, respectively, and K_p, K_v, and K_i diagonal positive definite matrices. Let the error vector E and its derivative be:

$$E = \theta_d - \theta;\ \dot{E} = \dot{\theta_d} - \dot{\theta},\ \ddot{E} = \ddot{\theta_d} - \ddot{\theta} \tag{6}$$

Therefore, relation (5) can be rewritten in the following form:

$$\ddot{E} + K_v\dot{E} + K_pE + K_i \int E\, dt = 0 \tag{7}$$

Therefore, a proper choice of these matrices ensures the stability of the system.

B. Sliding Mode Control(SMC)

The general layout of the SMC is depicted in Fig. 3. The first step in the sliding mode control is to choose the sliding (or switching) surface S in terms of the tracking error. Let the tracking error for each joint be defined as:

$$e_i = \theta_i - \theta_i^d \quad \cdots \quad (i = 1, \cdots, m) \tag{8}$$

and the sliding surface as:

$$S_i = \lambda_i e_i + \dot{e}_i \quad \cdots \quad (i = 1, \cdots, m) \tag{9}$$

where, θ_i^d is the desired trajectory for joint i, and S_i is the sliding surface of each DoF.

Let, $\Sigma = [S_1 \quad S_2 \quad \cdots \quad S_m]^T$ be the sliding surface for the developed *MARSE*. Therefore, we have —

$$\Sigma = \begin{bmatrix} \lambda_1 e_1 + \dot{e}_1 \\ \vdots \\ \lambda_m e_m + \dot{e}_m \end{bmatrix} \tag{10}$$

Equation (10) is a first order differential equation, which implies that if the sliding surface is reached, the tracking error will converge to zero as long as the error vector stays on the surface. Considering the following Lyapunov function candidate:

$$V = \frac{1}{2}\Sigma^T\Sigma \tag{11}$$

which is continuous and nonnegative. The derivative of V yields:

$$\dot{V} = \Sigma^T\dot{\Sigma} \tag{12}$$

By choosing $\dot{\Sigma}$ as given in (13) relation (12) is ensured to be decreasing.

$$\dot{\Sigma} = -K\ sign(\Sigma)\ ,\ \forall t, K > 0 \ \Rightarrow\ \dot{V} < 0 \tag{13}$$

where,

$$sign(\Sigma) = \begin{cases} 1\ for\ \Sigma > 0 \\ 0\ for\ \Sigma = 0 \\ -1\ for\ \Sigma < 0 \end{cases} \tag{14}$$

Expression (13) is known as the reaching law. It is to be noted that the discontinuous term $K\ sign(\Sigma)$ in (13) often leads to a high control activity, known as chattering. In most systems, the chattering phenomenon is undesirable, because it can excite high frequency dynamics which could be the cause of severe damage. One of the most known approaches found in the literature is to smoothen the discontinuous term in the control input with the continuous term $K\ sat(\Sigma/\phi)$ [10].

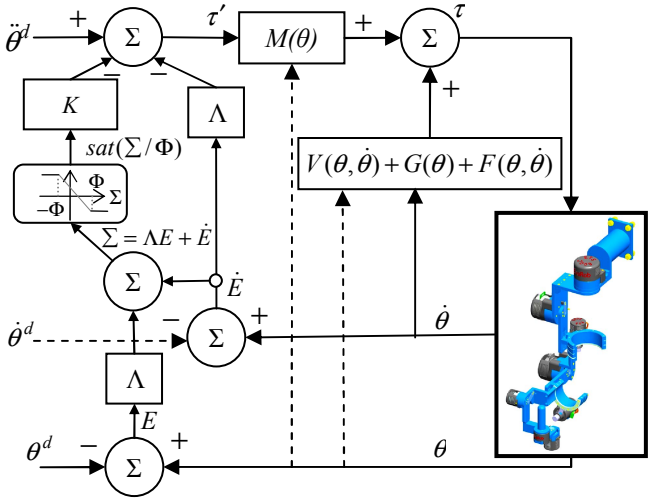

Fig. 3. Schematic diagram of SMC

where

$$sat(\Sigma/\phi) = \begin{cases} 1\ for \dfrac{\Sigma}{\phi} > 1 \\ \dfrac{\Sigma}{\phi}\ for -1 \le \dfrac{\Sigma}{\phi} \le 1 \\ -1\ \text{Otherwise} \end{cases} \quad \forall t, 0 < \phi \ll 1 \tag{15}$$

Using equation (15), the reaching law therefore becomes:

$$\dot{\Sigma} = -K\ sat(\Sigma/\phi)\ ,\ \forall t, K > 0 \tag{16}$$

Therefore and considering:

$$\ddot{\theta}^d = [\ddot{\theta}_1^d \quad \ddot{\theta}_2^d \quad \ldots \quad \ddot{\theta}_m^d]^T,$$

$$\dot{E} = [\dot{e}_1 \quad \dot{e}_2 \quad \cdots \quad \dot{e}_m]^T, \text{ and } \Lambda = \begin{bmatrix} \lambda_i & 0 & 0 \\ 0 & \ddots & 0 \\ 0 & 0 & \lambda_m \end{bmatrix}.$$

Equation (10), therefore can be written as:

$$\Sigma = \Lambda E + \dot{E} \quad \Rightarrow \quad \dot{\Sigma} = \Lambda\dot{E} + \ddot{E} \tag{17}$$

where $\ddot{E} = \ddot{\theta} - \ddot{\theta}^d$. Thus, relation (17) can be written as:

$$\dot{\Sigma} = \Lambda\dot{E} + \ddot{\theta} - \ddot{\theta}^{d} \tag{18}$$

Substituting the value of $\ddot{\theta}$ from (3) in (18) we obtain,

$$\dot{\Sigma} = \Lambda\dot{E} - \ddot{\theta}^{d} - M^{-1}(\theta)\big[V(\theta,\dot{\theta}) + G(\theta) + F(\theta,\dot{\theta})\big] + M^{-1}(\theta)\tau \tag{19}$$

Replacing $\dot{\Sigma}$ by its value given in (16)

$$-K\ sat(\Sigma/\phi) = \Lambda\dot{E} - \ddot{\theta}^{d} - M^{-1}(\theta)\big[V(\theta,\dot{\theta}) + G(\theta) + F(\theta,\dot{\theta}) - \tau\big] \tag{20}$$

The torque τ can be isolated and thus yields:

$$\tau = -M(\theta)\left(\Lambda\dot{E} - \ddot{\theta}^{d} + K.sat(\Sigma/\phi)\right) + \big[V(\theta,\dot{\theta}) + G(\theta) + F(\theta,\dot{\theta})\big] \tag{21}$$

where K and Λ are diagonal positive definite matrices. Therefore, the control law given in (21) ensures that the control system is stable.

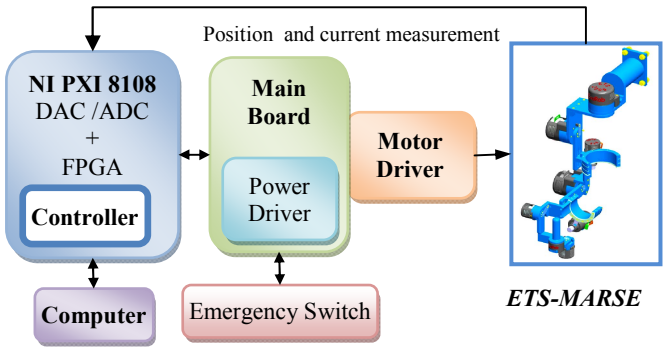

Fig. 4. Experimental setup.

IV. Experiments and Results

Experimental set up of the *ETS-MARSE* system is depicted in Fig. 4. It consists of a CPU processor (NI PXI-8108) with a reconfigurable FPGA (field-programmable gate array), a main board, seven motor driver cards, and a host PC. The control algorithm is executed in PXI-8108. The outputs of the controllers are the joints torque commands. However, the torque commands are converted to motor currents, and finally, to reference voltage as the voltage value is the drive command for the motor drivers. Note that the controllers update the torque commands every 0.5 ms. The control parameters (gains) used for the experiments were found by trial and error, and are as follows:

- CTC:

$K_v = diag[1.5 \quad 1.5 \quad 1.0 \quad 2.5 \quad 1.0 \quad 5.0 \quad 7.0]*100,$

$K_p = diag[18 \quad 25 \quad 20 \quad 45 \quad 90 \quad 150 \quad 200]*100,$

$K_i = diag[15 \quad 28 \quad 18 \quad 42 \quad 90 \quad 150 \quad 200]*100.$

- SMC:

$\Lambda = diag[15 \quad 15 \quad 15 \quad 15 \quad 15 \quad 10 \quad 10],$

$K = diag[350 \quad 300 \quad 330 \quad 550 \quad 2200 \quad 3000 \quad 3700].$

The mass and inertia properties of the *ETS-MARSE* were estimated from the CAD model using Pro/Engineer software. The dynamic model of the system also includes mass and inertial properties of adult male arm's model.

The experiments were conducted on healthy subjects (nos.: 4; age: 28 ± 4 years; height: 177 ± 8 cm; weight: 81 ± 17 kg) in a seated position. In experiments, trajectories tracking representing typical passive rehabilitation exercises [11] for single e.g., elbow flexion/extension and multi joint movements (e.g., reaching) were performed. Note that the reference (desired) trajectories and associated velocities were generated using a cubic polynomial approach [12].

A typical rehabilitation exercise involving elbow joint flexion extension movement is depicted in Fig. 5. The exercise began with the elbow joint at 90°. The topmost plot of the Fig. 6 compares the desired joint angles (or reference trajectories, dotted line) to measured joint angles (or measured trajectories, solid line). The 2nd row of the plot shows the tracking error of each joint movement as a function of time (i.e., deviation between desired and measured trajectories). The trials were performed with both SMC and CTC controls. It can be seen from the plots that the tracking error was quite small (<0.45°) Comparing Fig.5a with Fig. 5b, it can be seen that with the SMC technique, the maximum tracking error was around 0.20°, whereas with CTC it was around 0.45°.

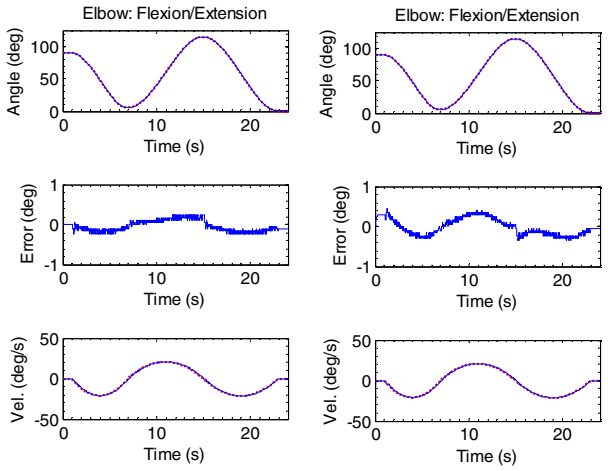

(a) (b)

Fig. 5. Elbow flextion/extension performed at a slow speed (max.25°/s). (a) SMC, (b) CTC.

Depending on the needs of patients, it is often required to change the speed of such exercises. Fig. 6 shows the similar exercises of Fig. 5 but were performed at a faster speed. The maximum velocity observed in this case was 60°/s. The bottom row of the plots displays velocity tracking (where the solid line indicates measured velocity and dotted line indicates desired velocity). As in the previous trials, the two controllers showed excellent tracking performance with tracking error limited to less than 0.75°. To further compare the performance of these controllers, similar exercises were performed with PID controller. Results of those trials are depicted in Fig. 7. Control gains for PID controllers are as follows:

$K_v = diag[30 \quad 25 \quad 10 \quad 35 \quad 10 \quad 5.0 \quad 5.0],$

$K_p = diag[250 \quad 550 \quad 100 \quad 500 \quad 250 \quad 70 \quad 30],$

$$K_i = diag[40 \quad 250 \quad 25 \quad 400 \quad 100 \quad 40 \quad 10].$$

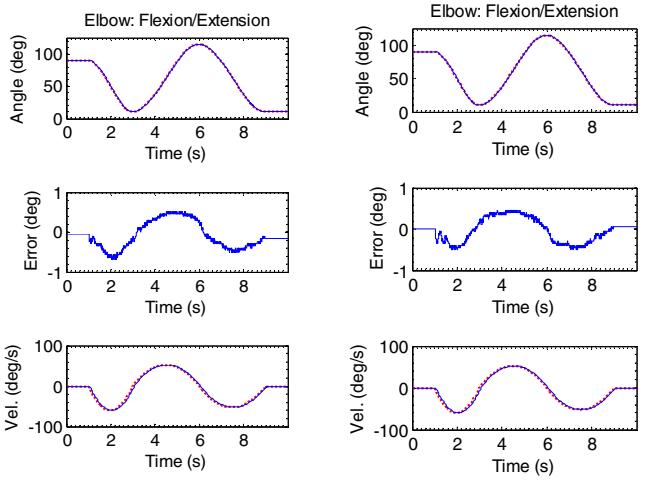

(a) (b)

Fig. 6. Elbow flexion/extension performed at a faster speed (max. 60°/s). (a) SMC (b) CTC

Compared to Fig.7 with Figs, 5 and 6, it can be found that with the PID control technique, the maximum tracking error was around 1.0°, whereas with CTC/SMC it was below 0.75°. However, from Figs. 5 and 6, we may conclude that at a variety of speeds both the controllers demonstrated excellent tracking performance, thus said to be adequate to provide passive arm movement therapy.

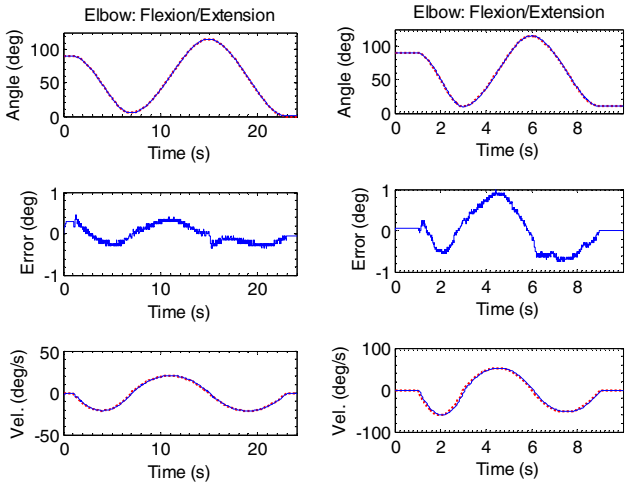

Fig. 7. Elbow flextion/extension performed with PID control

Fig. 8 shows the schematic diagram of another typical rehabilitation exercise involving simultaneous motions of the elbow and forearm. The objective of this exercise is to pronate the forearm from its initial position (0°) to the fully pronated position, while simultaneously flexing the elbow from its initial position (90°) to complete extension and next, inversely moving the forearm from full pronation to a full supinated position, while the elbow simultaneously goes from complete extension to complete flexion. Fig. 9 shows the experimental result of this exercise which was performed with SMC. Note that to evaluate the robustness of the controller this exercise

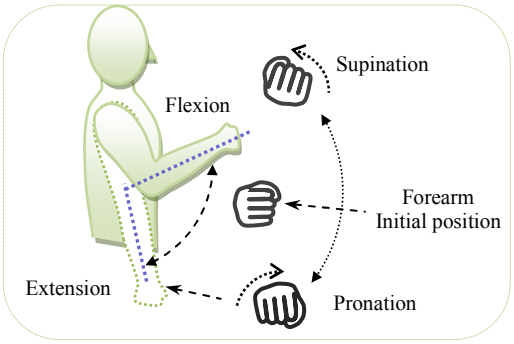

Fig. 8. Simultaneous movement of elbow and forearm

was performed at a much faster speed (observed maximum velocity: 100°/sec). The maximum tracking error observed in this case was found at the level of pronation /supination motion which was around 2.5°.

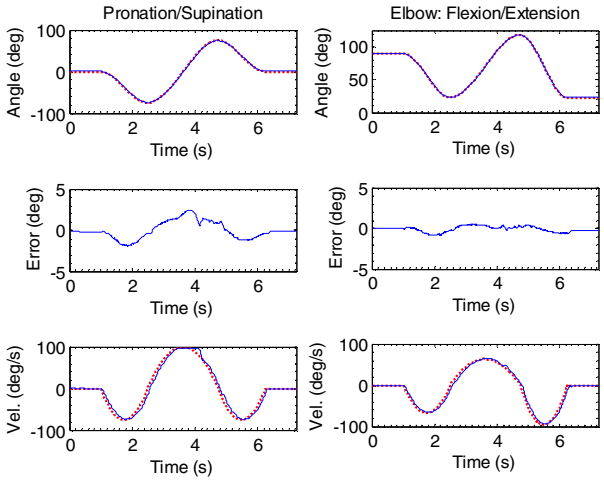

Fig. 9. Simultaneous motion of elbow and forearm, SMC

Note that for the same passive exercises were performed with the CTC and PID control techniques are depicted in Figs. 10 and 11 respectively. With CTC and PID controls, the maximum tracking error was also observed at the level of

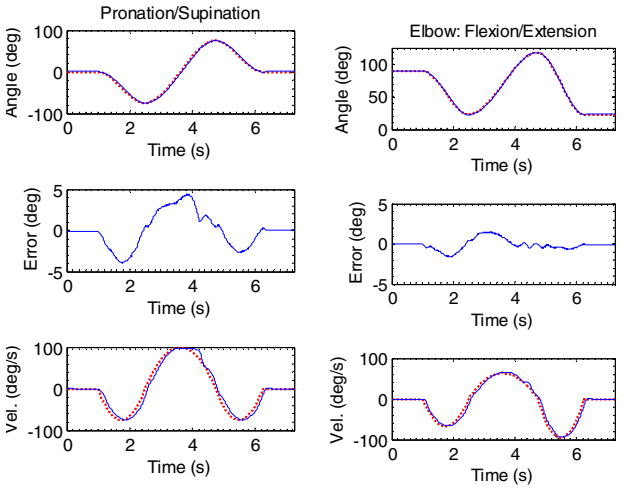

Fig. 10. Simultaneous motion of elbow and forearm, CTC

pronation /supination motion which was around 4.5° with the CTC and 3.5° with the PID. The noticeable feature of these experimental results is that unlike the single joint movement exercises as depicted in Figs. 5 -7 where CTC showed better tracking compared to PID, in this case (Fig.11) where multi-joints movements were involved PID showed better tracking compared to CTC.

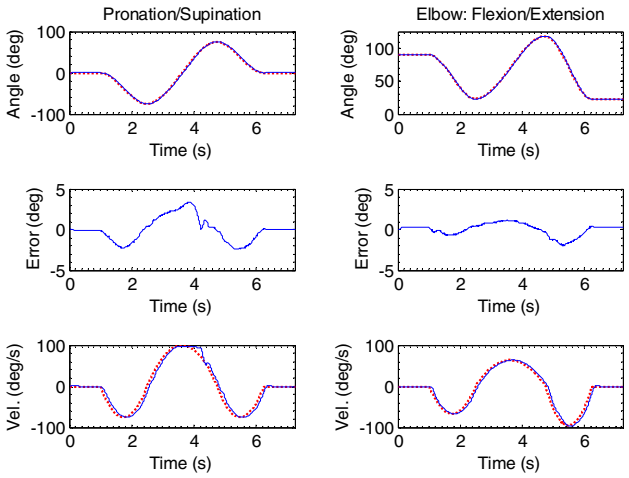

Fig. 11. Simultaneous motion of elbow and forearm, PID

Experimental results thus demonstrate that the SMC and the CTC can effectively maneuver the *ETS-MARSE* to provide passive arm movement therapy. These control techniques are robust and simple to design. The performance of the PID controller was also impressive even in the case of fast speed and showed better and smoother tracking compared to CTC. Theoretically, with perfect dynamic modeling, CTC should give better tracking performance compared to PID control when the *ETS-MARSE* is maneuvered at a high speeds. However, in practice it is difficult to estimate or find exact dynamic parameters. Moreover, it is challenging to model the nonlinear friction terms. Therefore, while using a nonlinear control approach, it was often necessary to simplify the dynamic model. Indeed, we did so in the dynamic modeling of the *ETS-MARSE* using the following strategies:

- using only the diagonal elements (i.e., Ixx , Iyy, and Izz) of the inertial terms.
- assuming that the structure of the *ETS-MARSE* arm is symmetric.
- modeling of the viscous friction term was ignored, considering the exercises will be performed at a low speed (passive rehabilitation therapy exercises should be performed slowly because of the subject's arm impairment).

V. Conclusions

Trajectory tracking corresponding to widely used passive rehabilitation exercises were implemented with a wearable upper limb 7DoFs exoskeleton robot, *ETS-MARSE*. A brief description of the *ETS-MARSE* is presented. In the experiments, tracking performance of the nonlinear computed torque control and sliding mode control was evaluated. Experimental results demonstrate the efficient performance of both control techniques (SMC and CTC) in maneuvering the *ETS-MARSE* as well as to provide passive arm movement therapy.

Future work will include developing a control strategy to provide active arm movement therapy using skin surface electromyogram signals [13].

Acknowledgment

The first author gratefully acknowledges the support provided for this research through a FRQNT-B3 scholarship.

References

[1] *Tracking Heart Disease and Stroke in Canada*: Public Health Agency of Canada, 2009.

[2] Heart & Stroke Foundation. (2009, August 25, 2010). *Tracking Heart Disease and Stroke in Canada*. Available: http://www.heartandstroke.com, [Accessed: 12 / 01/ 2013].

[3] P. A. Heidenreich, et al., "Forecasting the Future of Cardiovascular Disease in the United States A Policy Statement From the American Heart Association," *Circulation,* vol. 123, pp. 933-944, Mar 1 2011.

[4] G. Kwakkel, B. J. Kollen, J. van der Grond, and A. J. Prevo, "Probability of regaining dexterity in the flaccid upper limb: impact of severity of paresis and time since onset in acute stroke," *Stroke,* vol. 34, pp. 2181-6, Sep 2003.

[5] S. Masiero, A. Celia, G. Rosati, and M. Armani, "Robotic-assisted rehabilitation of the upper limb after acute stroke," *Arch Phys Med Rehabil,* vol. 88, pp. 142-149, Feb 2007.

[6] M. H. Rahman, T. K. Ouimet, M. Saad, J. P. Kenne, and P. S. Archambault, "Dynamic Modeling and Evaluation of a Robotic Exoskeleton for Upper-Limb Rehabilitation," *International Journal of Information Acquisition,* vol. 8, pp. 83-102, 2011.

[7] M. H. Rahman, T. K. Ouimet, M. Saad, J. P. Kenne, and P. S. Archambault, "Development of a 4DoFs Exoskeleton Robot for Passive Arm Movement Assistance," *Int. J. Mechatronics and Automation,* vol. 2, pp. 34-50, 2012.

[8] M. H. Rahman, T. K. Ouimet, M. Saad, J. P. Kenne, and P. S. Archambault, "Development and Control of a Robotic Exoskeleton for Shoulder, Elbow and Forearm Movement Assistance," *Applied Bionics and Biomechanics,* vol. 9, pp. 275-292, 2012.

[9] N. F. Gordon, M. Gulanick, F. Costa, G. Fletcher, B. A. Franklin, E. J. Roth, and T. Shephard, "Physical activity and exercise recommendations for stroke survivors: an American Heart Association scientific statement from the Council on Clinical Cardiology, Subcommittee on Exercise, Cardiac Rehabilitation, and Prevention; the Council on Cardiovascular Nursing; the Council on Nutrition, Physical Activity, and Metabolism; and the Stroke Council," *Stroke,* vol. 35, pp. 1230-1240, May 2004.

[10] J. J. E. Slotine and W. Li, *Applied nonlinear control*. Englewood Cliffs, N.J.: Prentice-Hall, 1991.

[11] Department of Rehabilitation Services, Brigham and Women's Hospital *Physical Therapy Standards 2011*. Available: http://www.brighamandwomens.org/Patients_Visitors/pcs/rehabilitationservices/StandardsofCare.aspx, [Accessed: 27 / 03/ 2013]

[12] J. J. Craig, *Introduction to robotics : mechanics and control*, 3rd ed. Upper Saddle River, N.J.: Pearson/Prentice Hall, 2005.

[13] K. Kiguchi, M. H. Rahman, M. Sasaki, and K. Teramoto, "Development of a 3DOF mobile exoskeleton robot for human upper-limb motion assist," *Robotics and Autonomous Systems,* vol. 56, pp. 678-691, Aug 31 2008.